

Performance Guarantees for Spectral Initialization in Rotation Averaging and Pose-Graph SLAM

Kevin J. Doherty^{*1}, David M. Rosen², and John J. Leonard¹

¹*Computer Science and Artificial Intelligence Laboratory, Massachusetts Institute of
Technology, Cambridge, MA 02139, USA*

²*Laboratory for Information and Decision Systems, Massachusetts Institute of Technology,
Cambridge, MA 02139, USA*

Abstract

In this work we present the first initialization methods equipped with *explicit performance guarantees* that are adapted to the pose-graph simultaneous localization and mapping (SLAM) and rotation averaging (RA) problems. SLAM and rotation averaging are typically formalized as large-scale nonconvex point estimation problems, with many bad local minima that can entrap the smooth optimization methods typically applied to solve them; the performance of standard SLAM and RA algorithms thus crucially depends upon the quality of the estimates used to initialize this local search. While many initialization methods for SLAM and RA have appeared in the literature, these are typically obtained as purely heuristic approximations, making it difficult to determine whether (or under what circumstances) these techniques can be reliably deployed. In contrast, in this work we study the problem of initialization through the lens of *spectral relaxation*. Specifically, we derive a simple spectral relaxation of SLAM and RA, the form of which enables us to exploit classical linear-algebraic techniques (eigenvector perturbation bounds) to control the distance from our spectral estimate to *both* the (unknown) ground-truth *and* the global minimizer of the estimation problem as a function of measurement noise. Our results reveal the critical role that spectral graph-theoretic properties of the measurement network play in controlling estimation accuracy; moreover, as a by-product of our analysis we obtain new bounds on the estimation error for the *maximum likelihood* estimators in SLAM and RA, which are likely to be of independent interest. Finally, we show experimentally that our spectral estimator is very effective in practice, producing initializations of comparable or superior quality at lower computational cost compared to existing state-of-the-art techniques.

^{*}Corresponding author. Email: kjd@csail.mit.edu

Contents

1	Introduction	3
2	Related work	4
3	Preliminaries and formulation	5
3.1	Notation and preliminaries	5
3.2	Problem formulation	6
4	Spectral methods for initialization	7
5	Main results	9
6	Experimental results	12
6.1	Evaluation on synthetic data	13
6.2	Evaluation on standard SLAM benchmark datasets	14
7	Conclusion	16
A	Structure of the data matrices	17
B	Analysis of the spectral relaxation	18
B.1	Recovering minimizers of Problem 4 as eigenvectors	18
B.2	Symmetric perturbations of symmetric matrices	19
C	Proof of the main results	19
C.1	An upper bound for the estimation error in Problem 4	20
C.2	An upper bound for the estimation error in Problem 3	21
C.3	An upper bound on $d_{\mathcal{S}}(R^{(0)}, R^*)$	23
D	Relationship to the method of Moreira et al. [22]	24

1 Introduction

Simultaneous localization and mapping (SLAM) is the process by which a robot jointly infers its pose and the location of environmental landmarks; this is a fundamental capability of mobile robots, supporting navigation, planning, and control [26]. State-of-the-art methods typically formalize SLAM and rotation averaging as large-scale M-estimation problems, and then apply smooth first- or second-order local optimization methods to efficiently recover a point estimate. However, the fact that robot orientations are elements of the special orthogonal group $SO(d)$, a nonconvex set, makes these estimation problems inherently *nonconvex*, with many bad local minima that can entrap the local optimization methods commonly applied to solve them. The performance of standard SLAM and RA algorithms thus crucially depends upon the quality of the estimates used to initialize the local search. In consequence, a great deal of prior work has been dedicated to the development of initialization techniques (see Carlone et al. [10] for a review). While many of these techniques often work well in practice, the fact that they are obtained as heuristic approximations makes it difficult to ascertain *what specific features* of SLAM or RA problems determine their performance. As a result, it is difficult to say when, or under what conditions, these techniques can be *reliably* deployed.

In this work, we propose a simple *spectral initialization* method for pose-graph SLAM and rotation averaging that we prove enjoys *explicit performance guarantees*. To the best of our knowledge, these are the first concrete guarantees to appear in the literature for any initialization technique adapted to these applications. Our analysis gives direct control over the estimation error of a spectral initialization in terms of the spectral properties of the measurement network.¹ This allows us to control the distance from the spectral estimate to the global minimizer of the estimation problem; this is critical for ensuring that the initialization lies in the locally convex region around the global minimizer, and therefore that this minimizer can be recovered by a subsequent local refinement (see Figure 1). Our proof of this result relies on new estimation error bounds for the global minimizers (i.e. the *maximum likelihood* estimators) of SLAM and rotation averaging problems, which are likely to be of independent interest. Algorithmically, our approach only requires computing the first few eigenpairs of a symmetric matrix, which can be achieved using any off-the-shelf implementation of the Lanczos method (e.g. the MATLAB `eigs` command). Our empirical results on both synthetic data and standard pose-graph SLAM benchmarks demonstrate that the spectral estimator typically performs far better than our worst-case analysis suggests, achieving solution quality and computation times competitive with state-of-the-art approaches. Beyond its utility as an *initialization method* for M-estimation, our results show that spectral relaxation provides an inexpensive method for rotation averaging and pose-graph optimization in its own right (i.e. *without* the need to perform subsequent nonconvex optimization or semidefinite relaxation) that attains an asymptotic error bound comparable to the (globally optimal) M-estimator, and provides near-optimal estimates in practice.

The remainder of the paper proceeds as follows: In Section 2, we discuss related literature on robot perception and rotation averaging. Section 3 formalizes the estimation problem, and Section 4 describes our spectral initialization procedure. In Section 5 we present our main results: an analysis controlling the estimation error of both the spectral initialization and the global minimizer for the rotation averaging and pose-graph SLAM problems, as well as a bound on the distance between the spectral initialization and the globally optimal solution. Section 6 demonstrates the empirical performance of our spectral estimator on benchmark SLAM datasets, together with our performance bound evaluated on synthetic data. These results show, in particular, that the spectral estimator is competitive with state-of-the-art techniques for initialization.

¹Recent work has identified spectral properties of measurement networks as key quantities controlling the performance of estimators for these problems, though this connection (particularly in the context of SLAM) remains under-explored (see [26] for a recent review).

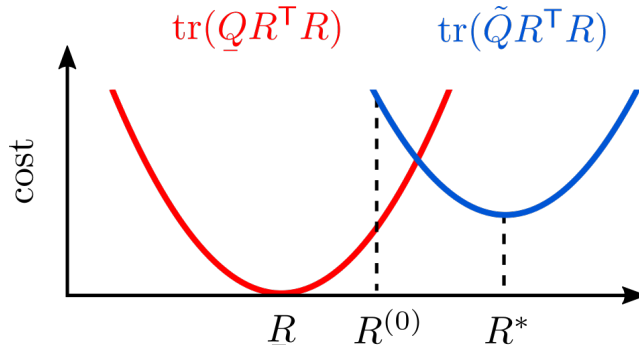


Figure 1: **Comparing true, optimal, and initial rotation estimates.** We are interested in bounds on the deviation of an initial estimate $R^{(0)}$ from the (latent) ground truth \underline{R} and the globally optimal solution R^* .

2 Related work

Simultaneous localization and mapping and rotation averaging problems are often formulated as high-dimensional, nonconvex optimization problems. Consequently, solving these problems typically requires efficient algorithms for producing an “initial guess.” Historically, research on this topic has focused on developing cheap, but typically inexact, convex or linear relaxations of the SLAM (resp. rotation averaging) problems (e.g. [10, 21]). While these techniques often work well in practice, the fact that they are obtained as heuristic approximations makes it difficult to ascertain *what specific features* of SLAM or RA problems determine their performance. Consequently, it is difficult to assess *under what conditions* these techniques can be reliably deployed.

A related line of research is the development of Cramér-Rao bounds for the pose-graph SLAM and rotation averaging problems [7, 12, 18]; these works provide *lower bounds* on the achievable estimation error *in expectation*. In this work, we derive a complementary set of *upper bounds* on the estimation error on a *per instance* basis. Interestingly, our estimation error *upper* bounds depend upon precisely the same spectral quantities as do the Cramér-Rao (*lower*) bounds, indicating that graph spectra are objects of central importance in understanding the statistical properties of SLAM and RA estimators.

The spectral relaxation approach to initialization that we consider has previously appeared in other problem settings, particularly in the area of phase synchronization problems (cf. [5, 6, 19, 27]). In particular, Ling [19] describe error bounds that are qualitatively similar to those described in this paper, though theirs are concerned specifically with *orthogonal* group synchronization problems. Liu et al. [20] take a similar approach to ours in order to derive error bounds for spectral estimators of synchronization problems defined over subgroups of the orthogonal group (including $\text{SO}(d)$), but employ a different definition of the perturbation than the one we consider here. As we will show, our notion of perturbation has the advantage that it follows naturally from a generative model of SLAM and RA, and furthermore, directly reveals the spectral properties of the measurement network (specifically, a kind of generalized algebraic connectivity) as the key quantities controlling the worst-case performance of our spectral initialization method.

Recently, Moreira et al. [22] proposed a computationally-efficient Krylov-Schur decomposition approach for pose-graph SLAM. We show in Appendix D that their method is formally equivalent to a *special case* of our approach (namely, an *unweighted, rotation-only* variant of our spectral initialization procedure). However, our construction arises more naturally from spectral relaxation, and additionally allows for the incorporation of translational measurements, which we show in Section 6 can have a significant impact on estimation quality. Arrigoni et al. [2] also

describe a spectral method for $\text{SE}(d)$ -synchronization. While an analysis similar to ours could likewise be carried out for their method, the form of the relaxation they consider would lead to more complicated bounds due to a dependence on the scale of the translational states. Finally, Boots and Gordon [4] consider spectral techniques for the range-only SLAM problem. Though their problem setting differs from the one considered here, extension of the techniques presented in this work to scenarios with different types of measurement models is an interesting area for future work.

Finally, *certifiably-correct* machine perception has emerged as a key area of interest to the robotics community, resulting in the development of algorithms capable of directly computing *globally optimal* solutions of certain nonconvex estimation problems under moderate noise [8, 9, 11, 13, 14, 25, 29]. Our analysis provides new bounds on the estimation error of the maximum likelihood estimators recovered by these techniques in terms of the magnitude of the measurement noise. Moreover, the bounds we present suggest that when these estimators, which are often based on large-scale semidefinite relaxations, do attain globally optimal solutions, the resulting estimates have error bounds that *match* (up to small constant factors) the error bounds we derive for our spectral initialization, which is easily implemented and computationally inexpensive.

3 Preliminaries and formulation

3.1 Notation and preliminaries

Lie groups and matrix manifolds: We will make use of the matrix realizations of several Lie groups, most prominently the d -dimensional special Euclidean and special orthogonal groups, denoted $\text{SE}(d)$ and $\text{SO}(d)$, respectively. $\text{SE}(d)$ can be realized as a matrix group according to:

$$\text{SE}(d) \triangleq \left\{ \begin{bmatrix} R & t \\ 0 & 1 \end{bmatrix} \in \mathbb{R}^{(d+1) \times (d+1)} \mid R \in \text{SO}(d), t \in \mathbb{R}^d \right\}, \quad (1)$$

and the group $\text{SO}(d)$ can be realized as:

$$\text{SO}(d) \triangleq \{R \in \mathbb{R}^{d \times d} \mid R^T R = I_d, \det(R) = 1\}, \quad (2)$$

where I_d is the $(d \times d)$ identity matrix. The *Stiefel manifold* $\text{St}(k, n)$ is the set of orthonormal k -frames in \mathbb{R}^n ($k \leq n$):

$$\text{St}(k, n) \triangleq \{V \in \mathbb{R}^{n \times k} \mid V^T V = I_k\}. \quad (3)$$

Linear algebra: For a symmetric matrix S , $S \succeq 0$ denotes that S is positive-semidefinite. The eigenvalues of a symmetric matrix $S \in \mathbb{R}^{n \times n}$ are denoted $\lambda_1(S) \leq \lambda_2(S) \leq \dots \leq \lambda_n(S)$. We will also consider several block-structured matrices, and make use of a few special operators acting on them. Following the notation of Rosen et al. [25], given square matrices $A_i \in \mathbb{R}^{d \times d}$, $i = 1, \dots, n$, we let $\text{Diag}(A_1, \dots, A_n)$ denote the matrix direct sum (i.e., the block-diagonal matrix having A_1, \dots, A_n as its diagonal blocks). Furthermore, given a block-structured matrix B , let $\text{BlockDiag}_d(B)$ denote the operator extracting a $d \times d$ block-diagonal matrix from B . Finally, let $\text{SBD}(d, n)$ denote the set of $dn \times dn$ symmetric block-diagonal matrices with diagonal blocks of size $d \times d$, and $\text{SymBlockDiag}_d(A)$ be the operator extracting the symmetrization of the $d \times d$ block-diagonal part of A .

Probability and statistics: We denote the multivariate Gaussian distribution with mean $\mu \in \mathbb{R}^d$ and covariance $\Sigma \in \mathbb{S}_+^d$ as $\mathcal{N}(\mu, \Sigma)$. We denote the isotropic Langevin distribution on

$\text{SO}(d)$ with mode $M \in \text{SO}(d)$ and concentration parameter $\kappa \geq 0$ as $\text{Langevin}(M, \kappa)$; this is the distribution whose probability density function is:

$$p(R; M, \kappa) = \frac{1}{c_d(\kappa)} \exp(\kappa \text{tr}(M^T R)), \quad (4)$$

with respect to the Haar measure on $\text{SO}(d)$, with $c_d(\kappa)$ a normalization constant.

Finally, for an unknown variable Z we aim to infer, we denote its true latent value by \underline{Z} and a noisy measurement of Z by \tilde{Z} .

Gauge-invariant distance metrics: A key property of rotation averaging and pose-graph optimization is that, as synchronization problems, they admit infinitely many solutions due to *gauge symmetry*. In particular, we will see that if $R^* \in \text{SO}(d)^n$ is an optimal estimate of the rotational states, then GR^* is also optimal for any $G \in \text{SO}(d)$. We therefore define the following *orbit distances* in order to compare solutions to the problems in a symmetry-aware manner:

$$d_S(X, Y) \triangleq \min_{G \in \text{SO}(d)} \|X - GY\|_F, \quad X, Y \in \text{SO}(d)^n \quad (5a)$$

$$d_O(X, Y) \triangleq \min_{G \in \text{O}(d)} \|X - GY\|_F, \quad X, Y \in \text{O}(d)^n. \quad (5b)$$

It will be convenient to “overload” the $\text{O}(d)$ orbit distance to act on elements of the set $\mathcal{Y} \triangleq \{Y \in \mathbb{R}^{d \times dn} \mid YY^T = nI_d\}$.² That is, for $X, Y \in \mathcal{Y}$:

$$d_O(X, Y) \triangleq \min_{G \in \text{O}(d)} \|X - GY\|_F. \quad (6)$$

Each of these distances can be computed in closed form by means of a singular value decomposition (see Rosen et al. [25, Theorem 5]).

3.2 Problem formulation

We consider the problem of synchronization over the $\text{SO}(d)$ group: this is the problem of estimating n unknown values $R_1, \dots, R_n \in \text{SO}(d)$ given a set of noisy measurements \tilde{R}_{ij} of a subset of their pairwise relative rotations $\underline{R}_{ij} \triangleq R_i^{-1} R_j$. The problem of $\text{SO}(d)$ -synchronization captures, in particular, the problems of rotation averaging and, under common modeling assumptions, pose graph optimization (as we show in Problem 3 and equation (PGO)), where the variables of interest are the orientations of a robot (or more generally, a rigid body) at different points in time (see, for example Grisetti et al. [15]). This problem possesses a natural graphical structure $\mathcal{G} \triangleq (\mathcal{V}, \mathcal{E})$, where nodes \mathcal{V} correspond to latent variables $R_i \in \text{SO}(d)$ and edges $(i, j) \in \mathcal{E}$ correspond to (noisy) measured relative rotations \tilde{R}_{ij} between R_i and R_j . In particular, for the problem of *rotation averaging*, we adopt the following standard generative model for rotation measurements: For each edge $(i, j) \in \mathcal{E}$, we sample a noisy relative measurement \tilde{R}_{ij} according to (cf. [13, 25]):

$$\tilde{R}_{ij} = \underline{R}_{ij} R_{ij}^\epsilon, \quad R_{ij}^\epsilon \sim \text{Langevin}(I_d, \kappa_{ij}). \quad (7)$$

Given a set of noisy pairwise relative rotations \tilde{R}_{ij} sampled according to the generative model (7), a maximum likelihood estimate $R^* \in \text{SO}(d)^n$ for the latent rotational states R_1, \dots, R_n is obtained as a minimizer of the following problem [13, 25]:

²The elements of \mathcal{Y} admit a straightforward interpretation as transposed and re-scaled elements of the Stiefel manifold $\text{St}(d, dn)$ (see (3)).

Problem 1 (Maximum likelihood estimation for rotation averaging).

$$\min_{R_i \in \text{SO}(d)} \sum_{(i,j) \in \tilde{\mathcal{E}}} \kappa_{ij} \|R_j - R_i \tilde{R}_{ij}\|_F^2. \quad (8)$$

For pose-graph SLAM (SE(d)-synchronization), we adopt the following generative model for rotation and translation measurements: For each edge $(i, j) \in \tilde{\mathcal{E}}$, we sample a noisy relative measurement $\tilde{x}_{ij} = (\tilde{t}_{ij}, \tilde{R}_{ij}) \in \text{SE}(d)$ according to:

$$\tilde{R}_{ij} = \underline{R}_{ij} R_{ij}^\epsilon, \quad R_{ij}^\epsilon \sim \text{Langevin}(I_d, \kappa_{ij}) \quad (9a)$$

$$\tilde{t}_{ij} = \underline{t}_{ij} + t_{ij}^\epsilon, \quad t_{ij}^\epsilon \sim \mathcal{N}(0, \tau_{ij}^{-1} I_d), \quad (9b)$$

where $x_{ij} = x_i^{-1} x_j = (\underline{t}_{ij}, \underline{R}_{ij})$ is the true relative transformation from x_i to x_j . Under this noise model, a maximum likelihood estimate $x^* \in \text{SE}(d)^n$ for the latent states x_1, \dots, x_n is obtained as a minimizer of the following problem [25]:

Problem 2 (Maximum likelihood estimation for SE(d) synchronization).

$$\min_{\substack{t_i \in \mathbb{R}^d \\ R_i \in \text{SO}(d)}} \sum_{(i,j) \in \tilde{\mathcal{E}}} \kappa_{ij} \|R_j - R_i \tilde{R}_{ij}\|_F^2 + \tau_{ij} \|t_j - t_i - R_i \tilde{t}_{ij}\|_2^2. \quad (10)$$

Note that under these modeling assumptions, both pose-graph optimization and rotation averaging can be written as particular instances of the following general optimization problem:

Problem 3 (Quadratic minimization over $\text{SO}(d)^n$).

$$p^* = \min_{R \in \text{SO}(d)^n} \text{tr}(\tilde{Q} R^\top R), \quad (11)$$

where $\tilde{Q} \in \text{Sym}(dn)$, $\tilde{Q} \succeq 0$.

Specifically, the problems of rotation averaging (RA) and pose-graph optimization (PGO) in Problems 1 and 2, respectively, can be parameterized in terms of the following data matrices:

$$\tilde{Q} = L(\tilde{G}^\rho), \quad (\text{RA})$$

$$\tilde{Q} = L(\tilde{G}^\rho) + \tilde{Q}^\tau, \quad (\text{PGO})$$

where $L(\tilde{G}^\rho)$ is the *rotation connection Laplacian* and \tilde{Q}^τ is a data matrix comprised of translation measurements. For the purposes of this paper, the specific structure of \tilde{Q} is not important; we require only that in the *noiseless case*, where $\tilde{Q} = Q$, we have $R^\top \in \ker(Q)$, where R is the set of (latent) ground-truth rotational states, and $L(G^\rho) \succeq 0$ and $Q^\tau \succeq 0$ (see [25, Appendix C.3] for a detailed analysis of the noiseless case). Finally, the interested reader may refer to Appendix A for a complete description of these data matrices.

4 Spectral methods for initialization

The nonconvexity of the $\text{SO}(d)$ constraint renders Problem 3 computationally hard to solve in general. However, we can generate a tractable *spectral relaxation* of Problem 3 by relaxing the $\text{SO}(d)$ constraint as follows:

Algorithm 1 Spectral initialization procedure

Input: The data matrix \tilde{Q} from (RA) or (PGO)

Output: A spectral initialization $R^{(0)}$

- 1: **function** SPECTRALINITIALIZATION(\tilde{Q})
 - 2: Compute orthogonal set of eigenvectors Y^* corresponding to the d smallest eigenvalues of \tilde{Q} . ▷ Solve Problem 4.
 - 3: **for** $i = 1, \dots, n$ **do**
 - 4: Set $R_i^{(0)} \leftarrow \Pi_S(Y_i^*)$, where Y_i^* is the i -th $(d \times d)$ block of Y^* . ▷ Definition 1
 - 5: **end for**
 - 6: **return** $R^{(0)}$
 - 7: **end function**
-

Problem 4 (Spectral Relaxation of Problem 3).

$$\begin{aligned}
 p_S^* &= \min_{Y \in \mathbb{R}^{d \times dn}} \text{tr}(\tilde{Q}Y^\top Y) \\
 \text{s.t. } &YY^\top = nI_d.
 \end{aligned} \tag{13}$$

Here, the $\text{SO}(d)$ constraint on each $(d \times d)$ block of the variable Y has been replaced by the (weaker) constraint that $YY^\top = nI_d$, i.e. the matrix Y is comprised of d orthogonal rows of norm \sqrt{n} . While the relaxed constraints in (13) are still quadratic and nonconvex, in Appendix B.1 we prove that a feasible point Y is a (*global*) minimizer of Problem 4 if and only if its rows are comprised of d pairwise orthogonal (and appropriately scaled) eigenvectors corresponding to the minimum d eigenvalues of \tilde{Q} . Therefore, one can recover an optimizer Y^* of Problem 4 via a simple eigenvector computation.³

For the noiseless problem parameterized by Q , the relaxation in Problem 4 is exact in the sense that $\underline{R} = GY^*$ for some $G \in \text{O}(d)$.⁴ This follows from the fact that, by construction, the ground truth rotations \underline{R}^\top lie in $\ker(Q)$,⁵ and $\underline{R}\underline{R}^\top = nI_d$ since $\underline{R} \in \text{SO}(d)^n$. Likewise, since \underline{R} is a minimizer of the relaxed problem *and* is in the feasible set for the Problem 3, it is also a minimizer for Problem 3. In general, however, we do not expect such a nice correspondence to hold. Indeed, a minimizer of Problem 4 need not even be *feasible* for Problem 3, since the former is obtained from the latter by relaxing constraints. Therefore, we must in general *round* the estimate provided by the spectral relaxation to obtain an approximate solution $R^{(0)} \in \text{SO}(d)^n$ in the feasible set of Problem 3. The following definition makes this precise.

Definition 1 (Projection onto $\text{SO}(d)$). For $X \in \mathbb{R}^{d \times d}$, the projection $\Pi_S(X)$ of X onto $\text{SO}(d)$ is by definition a minimizer of the following:

$$\min_{G \in \text{SO}(d)} \|X - G\|_F. \tag{14}$$

A minimizer for this problem is given in closed-form as [16, 30]:

$$\Pi_S(X) = U\Xi V^\top. \tag{15}$$

where $X = U\Sigma V^\top$ is a singular value decomposition, and Ξ is the matrix:

$$\Xi = \text{Diag}(1, 1, \det(UV^\top)). \tag{16}$$

³This justifies our referring to Problem 4 as a “spectral” relaxation of Problem 3.

⁴The spectral relaxation in Problem 4, like Problem 3, admits infinitely many solutions: if Y^* is a minimizer of Problem 4, then any GY^* , $G \in \text{O}(d)$ is also a minimizer.

⁵We refer the reader to [25, Appendix C.3] for detailed analysis of the noiseless case.

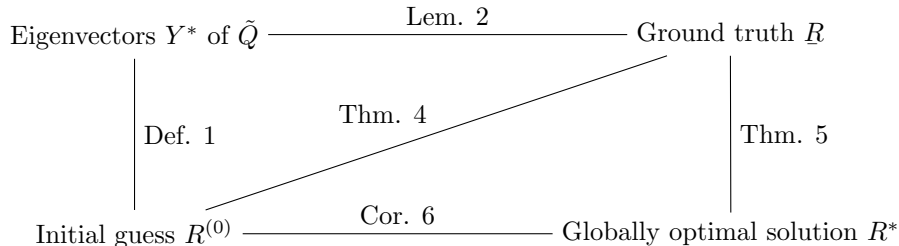


Figure 2: **Guide to the main results.** This figure presents a diagrammatic guide to the bounds presented in Section 5. Results here are represented by the edges between the quantities they relate. In particular, Lemma 2 gives a bound on the orbit distance between the eigenvectors of the data matrix and the ground truth. We then use this result in Theorem 4, giving a bound on the deviation of the spectral initialization from the ground truth. In Theorem 5 we bound the deviation of a *globally optimal solution* to the maximum likelihood estimation problems for rotation averaging and pose-graph SLAM from the ground truth. Finally, relating these bounds we obtain Corollary 6, which bounds the distance between a spectral initialization and the globally optimal solution.

In the context of subsequent derivations, it will be convenient to “overload” this rounding operation to $Y \in \mathbb{R}^{d \times dn}$ as follows:

$$\Pi_S(Y) = (\Pi_S(Y_1), \dots, \Pi_S(Y_n)), \quad (17)$$

where $Y_i \in \mathbb{R}^{d \times d}$ are the n blocks of Y .

Therefore, we can obtain an approximate solution to Problem 3 from a minimizer Y^* of the relaxation in Problem 4 as $R^{(0)} \triangleq \Pi_S(Y^*)$. Our overall spectral initialization procedure is summarized in Algorithm 1.

5 Main results

This section presents our main results, which are three-fold: First, we provide a bound on the error of our spectral initialization $R^{(0)}$ with respect to the ground-truth rotations R . Second, we give a new bound on the error of *globally optimal* solutions R^* with respect to R : this bound differs from prior work (e.g. Preskitt [23], Rosen et al. [25]) in that it is defined with respect to the orbit distance d_S on $\text{SO}(d)^n$. Previous work used the orbit distance $d_{\mathcal{O}}$ on $\text{O}(d)^n$ due to mathematical convenience; however, the estimation error one considers in application is actually over $\text{SO}(d)^n$, since this is the domain on which the estimation problem is defined. Combining these results, we obtain an upper bound on the $\text{SO}(d)$ orbit distance between an initial guess $R^{(0)}$ and a globally optimal solution R^* . Our analysis gives direct control over the mutual deviation between the three quantities of interest: $R^{(0)}$, R^* , and R as a function of the noise magnitude. We conclude with additional remarks about computing these bounds for practical SLAM scenarios and a few straightforward adaptations of the main results. Figure 2 gives an overview of the main results.

Recall from Problem 4 that an estimate Y^* is a minimizer of Problem 4 if and only if it is composed of a (suitably scaled) orthogonal set of eigenvectors corresponding to the minimum d eigenvalues of \tilde{Q} , and that in the noiseless case a minimizer is given by R . Since a spectral initialization $R^{(0)}$ is obtained as the projection of a solution Y^* of Problem 4 onto $\text{SO}(d)^n$, we can bound its estimation error by first bounding the deviation of Y^* from R , then bounding the additional error incurred by projecting onto $\text{SO}(d)^n$.

We will begin our presentation of the main results by giving a bound on the deviation of a solution Y^* of Problem 4 from the ground truth \underline{R} via the Davis-Kahan Theorem [31], a classical result relating the perturbation of a matrix's eigenvectors under a symmetric perturbation to the magnitude of that perturbation. Here, we take \underline{Q} to be the matrix under consideration, and define the perturbation $\Delta Q \triangleq \tilde{Q} - \underline{Q}$. The following lemma, which we prove in Appendix B.2, gives the desired characterization:

Lemma 2. *Let Y^* be a minimizer of Problem 4 and \underline{R} be the corresponding ground truth rotations. Then:*

$$d_{\mathcal{O}}(\underline{R}, Y^*) \leq \frac{2\sqrt{2dn}\|\Delta Q\|_2}{\lambda_{d+1}(\underline{Q})}. \quad (18)$$

Lemma 2 provides control over the deviation of an “unrounded” solution Y^* from the ground truth \underline{R} . The second technical ingredient we require is the following simple bound controlling the maximum distance between a matrix X and its projection $\Pi_{\mathcal{S}}(X)$ onto $\text{SO}(d)$:

Lemma 3. *Let $X \in \mathbb{R}^{d \times d}$ and $R \in \text{SO}(d)$. Then:*

$$\|\Pi_{\mathcal{S}}(X) - R\|_F \leq 2\|X - R\|_F. \quad (19)$$

Proof.

$$\|\Pi_{\mathcal{S}}(X) - R\|_F = \|\Pi_{\mathcal{S}}(X) - X + X - R\|_F \quad (20)$$

$$\leq \|\Pi_{\mathcal{S}}(X) - X\|_F + \|X - R\|_F \quad (21)$$

$$\leq 2\|X - R\|_F, \quad (22)$$

where the last inequality follows from the fact that $\Pi_{\mathcal{S}}(X)$ is a minimizer over $\text{SO}(d)$ of the distance to X with respect to the Frobenius norm, and that, by hypothesis, $R \in \text{SO}(d)$. \square

Lemma 3 provides a straightforward approach for converting a bound expressed in the $\text{O}(d)^n$ orbit distance to one expressed in the $\text{SO}(d)^n$ orbit distance. In turn, we obtain the following theorem, which we prove in Appendix C.1:

Theorem 4. *Let Y^* be a minimizer of Problem 4 and $R^{(0)} = \Pi_{\mathcal{S}}(Y^*) \in \text{SO}(d)^n$ be the corresponding spectral initialization. Finally, let $\underline{R} \in \text{SO}(d)^n$ be the set of ground truth rotations in Problem 3. Then the estimation error of $R^{(0)}$ satisfies:*

$$d_{\mathcal{S}}(\underline{R}, R^{(0)}) \leq \frac{4\sqrt{2dn}\|\Delta Q\|_2}{\lambda_{d+1}(\underline{Q})}. \quad (23)$$

The bound (23) gives a direct (linear) relationship between the magnitude of the perturbation ΔQ and the worst-case error of a spectral estimate. Moreover, Theorem 4 implies that $d_{\mathcal{S}}(\underline{R}, R^{(0)}) \rightarrow 0$ as $\Delta Q \rightarrow 0$. That is to say, as the measurements approach their noiseless counterparts, our spectral estimate approaches the ground truth.

Next, we address the issue of furnishing a bound on $d_{\mathcal{S}}(\underline{R}, R^*)$. The following theorem, which we prove in Appendix C.2, gives the desired result:

Theorem 5 (Bounding the estimation error for R^*). *Let R^* be a minimizer of Problem 3 and \underline{R} be the set of ground-truth rotations. Then the estimation error of R^* satisfies:*

$$d_{\mathcal{S}}(\underline{R}, R^*) \leq \frac{8\sqrt{dn}\|\Delta Q\|_2}{\lambda_{d+1}(\underline{Q})}. \quad (24)$$

To the best of our knowledge, Theorem 5 is the first result to appear in the literature that directly controls the estimation error of the maximum likelihood estimate R^* over $\text{SO}(d)^n$ specifically. Prior work considered the estimation error over $\text{O}(d)^n$ [3, 19, 25]. In our application, however, we are specifically concerned with the estimation error over $\text{SO}(d)^n$; as one can see from inspection, this is the domain on which Problem 3 is defined. Thus, the $\text{SO}(d)^n$ orbit distance corresponds to the actual error one would obtain in practice.

While Theorem 4 establishes error bounds for the spectral estimator, when viewed as an *initialization method*, the distance between the initial guess $R^{(0)}$ and the globally optimal solution is the primary concern. A corollary to Theorems 4 and 5, allows us to control $d_S(R^{(0)}, R^*)$ in terms of the noise matrix ΔQ . We have:

Corollary 6. *The orbit distance between the initialization $R^{(0)}$ and a globally optimal solution R^* satisfies:*

$$d_S(R^{(0)}, R^*) \leq \frac{(8 + 4\sqrt{2})\sqrt{dn}\|\Delta Q\|_2}{\lambda_{d+1}(Q)}. \quad (25)$$

These bounds provide a clear relationship between the spectral properties of Q and ΔQ and the deviation between a spectral estimator $R^{(0)}$, maximum likelihood estimator R^* , and the ground-truth R . An important consequence of these bounds is that as $\Delta Q \rightarrow 0$, we have (at least) linear convergence of the estimation error for *both* the spectral estimator and the maximum likelihood estimator to zero. This, in turn, guarantees that $\Delta Q \rightarrow 0$ implies $R^*, R^{(0)} \rightarrow R$ (up to symmetry), which is what we would expect.

In practice, however, we do not have access to Q . This presents some difficulty in the computation of ΔQ and $\lambda_{d+1}(Q)$. Fortunately, the noiseless rotation matrices admit a description in terms of quantities that *are* typically assumed to be known. In particular, we have [25, Lemma 8]:

$$\lambda_{d+1}(L(\mathcal{G}^\rho)) = \lambda_2(L(W^\rho)), \quad (26)$$

where $L(W^\rho)$ is the Laplacian of the rotational weight graph. Now, $L(W^\rho)$ depends only on the concentration parameters κ_{ij} attached to each edge, which are generally assumed to be known *a priori* from the noise models (7) and (9). In the rotation averaging case, we have $Q = L(\mathcal{G}^\rho)$, and therefore the denominator $\lambda_{d+1}(Q)$ is readily available as $\lambda_2(L(W^\rho))$, the algebraic connectivity of the rotational weight Laplacian.

In the case of pose-graph SLAM, where the matrix Q contains the translational terms Q^τ , we can use the fact that $Q = L(\mathcal{G}^\rho) + Q^\tau$ is the sum of positive-semidefinite matrices (see Rosen et al. [25, Appendix C.3]), so $\lambda_{d+1}(L(\mathcal{G}^\rho)) \leq \lambda_{d+1}(L(\mathcal{G}^\rho) + Q^\tau) = \lambda_{d+1}(Q)$. In particular, the (weaker) bounds obtained by substituting $\lambda_{d+1}(Q)$ with $\lambda_{d+1}(L(\mathcal{G}^\rho))$ in (23) and (24) hold.

Moreover, a common SLAM initialization technique is that of *rotation only initialization* – i.e., to compute the initializer $R^{(0)}$ using *only* the relative rotation measurements [10]. This can have computational advantages in practice since $L(\tilde{\mathcal{G}}^\rho)$ is generally *sparse*; the same cannot be said for the pose-graph SLAM data matrix \tilde{Q} , as it arises via analytic elimination of the translational states, in which case the resulting data matrix \tilde{Q} is formed as a (dense) generalized Schur complement [25, Appendix B]. Interestingly, for pose-graph SLAM, a spectral initialization $R^{(0)}$ computed using the eigenvectors of $L(\tilde{\mathcal{G}}^\rho)$ (i.e. ignoring Q^τ) attains the bound:

$$d_S(R, R^{(0)}) \leq \frac{4\sqrt{2dn}\|\Delta L(\tilde{\mathcal{G}}^\rho)\|_2}{\lambda_{d+1}(L(\mathcal{G}^\rho))}. \quad (27)$$

This bound holds by the same reasoning as Theorem 4, but with the consideration that $R^\top \in \ker(L(\mathcal{G}^\rho))$.

As a final consideration, typically we do not have access to ΔQ (if we did, we could recover the true data matrix Q as $\tilde{Q} - \Delta Q$). In consequence, we need a method to estimate the likely

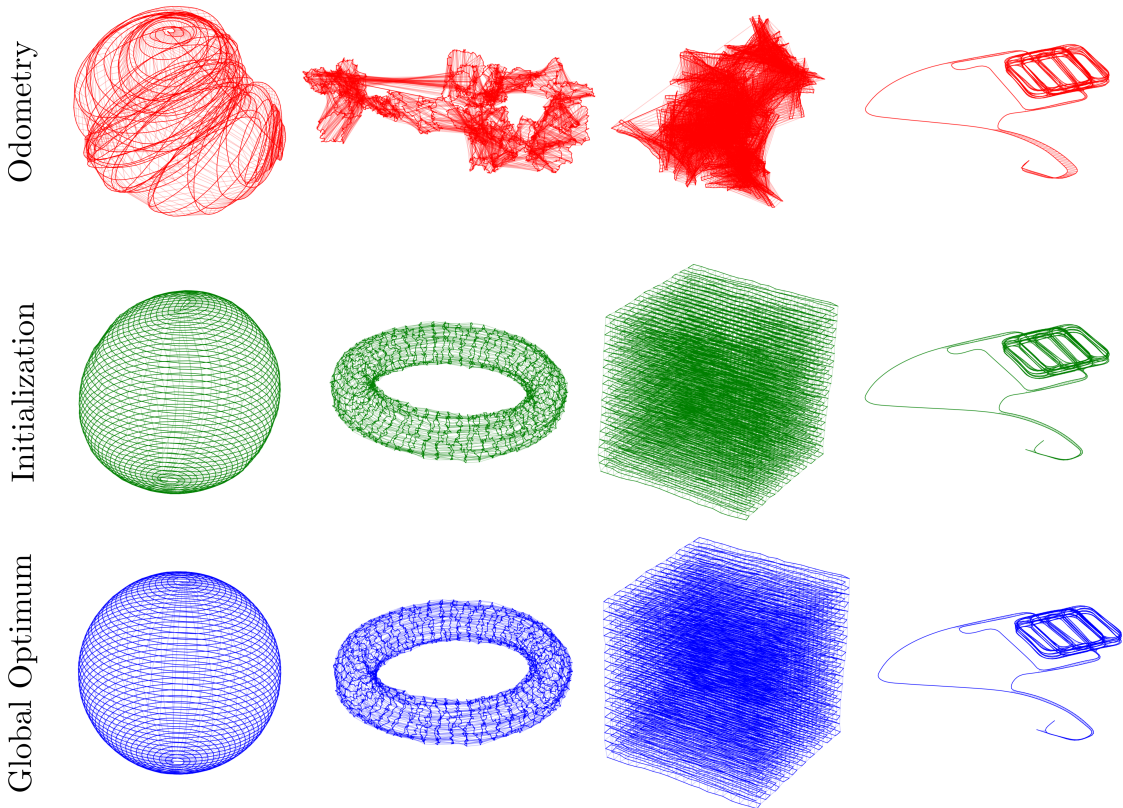


Figure 3: **Spectral relaxation produces high-quality initializations.** Qualitative comparison with the globally optimal solution suggests that the spectral relaxation produces estimates that are very close to optimal for a variety of SLAM benchmark datasets. The corresponding *quantitative* comparison is given in Table 1.

magnitude of the noise in a given application. One way of achieving this is via simulation from the generative model, given a measurement network and associated measurement precisions.⁶ This, in turn, gives a sample set from a *distribution* over the bounds (23), (24), and (25).

6 Experimental results

In this section, we compare the bounds in Theorem 4 to the actual estimation error incurred by the spectral initialization and globally optimal pose-graph SLAM solutions on a variety of simulated problem instances, as well as benchmark SLAM problems. In Section 6.1 we construct synthetic pose-graph SLAM scenarios for which the ground-truth poses are known. Since the bounds we have presented depend upon knowledge of the noise magnitude $\|\Delta Q\|_2$ and the spectral gap of the *true* data matrix Q , which are unknown in practice for pose-graph SLAM, our first set of empirical results shed light on the behavior of these worst-case bounds (as well as the *actual* error realized by different estimators) as we vary the noise parameters controlling the generative model (9). In Section 6.2, we evaluate the performance of spectral relaxation as a practical initialization

⁶Simulating measurements in the case of pose-graph SLAM requires knowledge of the ground-truth translation measurement scale, which is typically also unavailable in practice. However, the *rotation-only* initialization bound (27) applies in general and depends only upon the rotation measurements, which can be simulated to produce an empirical distribution over the spectral norm of the perturbation matrix.

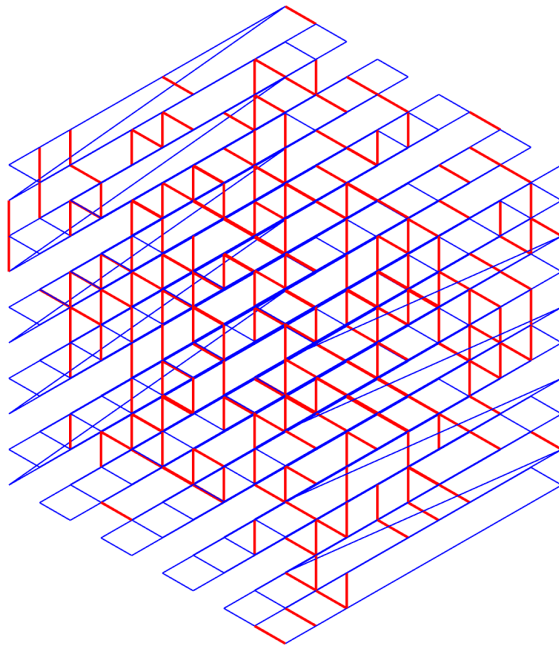


Figure 4: **Cube experiments.** Example ground-truth realization of a synthetic Cube dataset [9, 25] with $s = 10$ vertices per side and $p_{LC} = 0.1$. The robot’s trajectory is shown in blue with loop closures shown in red.

method in the context of 3D pose-graph SLAM applications. We show that, consistent with our results on synthetic data, the spectral initialization method offers high-quality initial solutions for pose-graph optimization, and in particular, that the inclusion of translational measurements significantly improves the quality of the spectral estimator versus the common approach of using exclusively rotational measurements.

The spectral initialization method was implemented in C++ using Spectra to efficiently solve large-scale eigenvalue problems [24]. Computation of the bounds in Section 6.1 was performed in MATLAB using `eigs`. All experiments were performed on a laptop with a 2.2 GHz Intel i7 CPU. Where (verified) globally optimal solutions were needed, we used the C++ implementation of SE-Sync [25]. We also provide results using the well-known *chordal* initialization method [21], which relaxes the feasible set of Problem 3 to $\mathbb{R}^{d \times dn}$, with the constraint that $R_1^{(0)} = I_d$, for which the solution can be obtained by solving a linear system.

6.1 Evaluation on synthetic data

The bounds presented in our analysis depend upon knowledge of the noise magnitude $\|\Delta Q\|_2$, which is unknown in practice. In light of this fact, we examine empirically the behavior of the bounds as a function of the noise parameters using synthetic data. Specifically, we use the Cube dataset [9, 25], which consists of a set of vertices (poses) organized in a three-dimensional cube, with s vertices per dimension. Consecutive poses have an “odometry” edge between them, and loop closures are sampled randomly from the remaining edges with probability p_{LC} . Measurements are generated by randomly sampling from the generative model (9) with fixed noise parameters κ and τ for all measurements. Beyond providing access to the ground-truth rotations, this setup allows us to compare the worst-case bounds with empirical performance in noise regimes well outside the range typically encountered in real SLAM scenarios. A sample

configuration for the Cube dataset is provided in Figure 4.

Influence of noise parameters on performance bounds: In Figure 5, we study the performance of the spectral initialization approach across a variety of noise configurations. In each case, we provide the worst-case bounds (23) and (27) along with the empirical error of the different estimators under consideration. In Figure 5a, we sample Cube problem instances with logarithmically spaced values of κ while fixing the other parameters: $\tau = 150$ (corresponding to an expected RMS error of 0.14 m), $p_{LC} = 0.2$, and $s = 10$. In Fig. 5b, we fix $\kappa = 10^5$ (corresponding to an expected RMS error of approximately 0.1°), $p_{LC} = 0.25$ and $s = 10$ and sample problem instances with logarithmically spaced translation concentration parameter τ . In Fig. 5c, we fix $\kappa = 10^5$, $\tau = 150$, $s = 10$ and vary p_{LC} from 0 to 1.

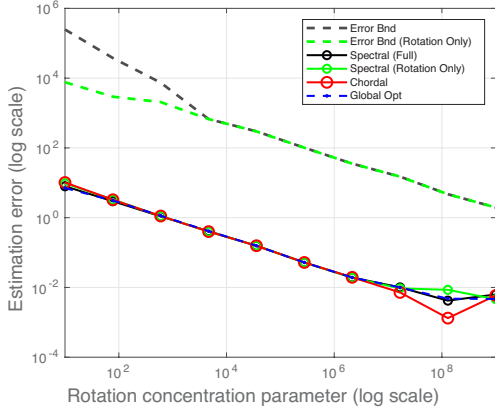
Across a wide range of concentration parameters, the spectral initializations attain very similar error to the global optimizer.⁷ In particular, their error often improves upon the worst-case bounds (23) and (27) by orders of magnitude. This is consistent with earlier observations of qualitatively similar bounds for phase synchronization [23]. Moreover, in applications of rotation averaging and pose-graph optimization, previous work has shown that the maximum likelihood estimator often attains expected error close to the Cramér-Rao *lower bound* (see [7] for rotation averaging and [12] for pose-graph optimization). The behavior of the bounds when varying the translation concentration parameter in Figure 5b is counterintuitive: while the spectral estimator improves with increasing τ , the bound suggests the opposite worst-case behavior. It seems the form of the bounds we derive (including the translational terms) is not refined enough to capture this behavior, and this certainly warrants further investigation. With this exception, the bounds seem to accurately capture the behavior of the actual estimation error.

Dependence on problem dimensionality: Due to the explicit appearance of the problem dimension n in the bounds (23), (24), and (25), it is interesting to consider how the number of rotations to be estimated affects these bounds. In Figure 5d, we fix $\kappa = 10^5$, $\tau = 150$, $p_{LC} = 0.2$ and vary the number of vertices in the Cube dataset. Indeed, we find that the behavior of the worst-case bounds suggests an unfavorable scaling in the problem dimension: at $s^3 = 8$ vertices, the worst-case bound overestimates the true error by approximately an order of magnitude; at $s^3 = 1000$, it overestimates the true error by approximately 3 orders of magnitude. It is unclear, at present, whether it is possible to remove this dependence on the problem dimension. A more sophisticated analysis considering the specific structure of these matrices (as defined in Appendix A) may yield more refined bounds.

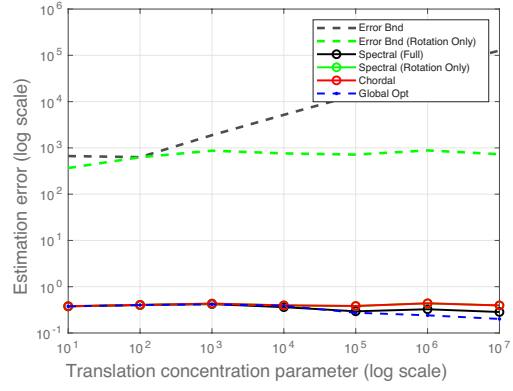
6.2 Evaluation on standard SLAM benchmark datasets

In these experiments, we consider evaluation of the spectral initialization method on several standard SLAM benchmark datasets. Figure 3 provides a qualitative comparison of three techniques for initialization: odometry only (i.e. composing measurements between consecutive poses), the proposed spectral initialization approach, and the globally optimal solution. We observe that spectral initialization provides solutions that visually resemble the globally optimal solution. Table 1 gives our quantitative results. For each method, we provide the computation time, objective value, and number of iterations required for a Riemannian trust-region (RTR) optimization method to converge to a critical point when using that initialization. With the exception of odometry-only initialization, all of the methods considered enabled the recovery of

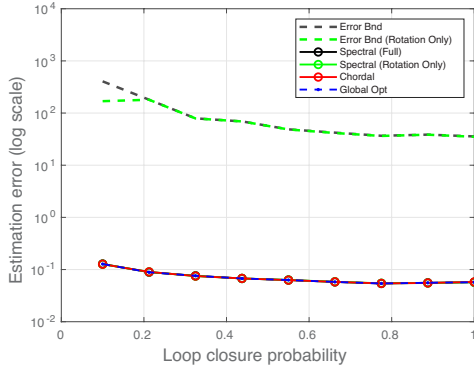
⁷ R^* is the maximum likelihood estimator—the optimal point estimate given the data. Since there is noise in the data, it is conceivable that the maximum likelihood estimate might actually be farther away from the ground truth than a “suboptimal” estimate, which we observe in Fig. 5a.



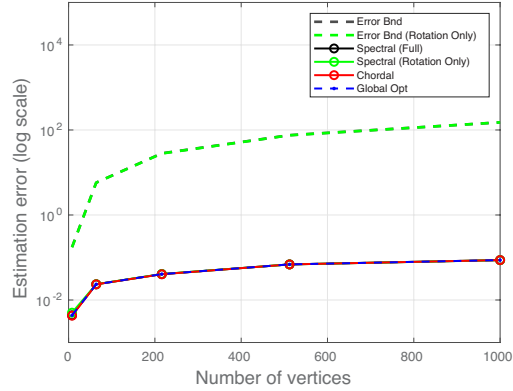
(a)



(b)



(c)



(d)

Figure 5: **Influence of dataset parameters on the performance bounds for the Cube experiments.** We examine empirically the change in the theoretical bounds (23) and (27) as well as the estimation error of several pose-graph optimization estimates while varying (a) the rotation concentration parameter κ , (b) the translation concentration parameter τ , (c) the probability of a loop closure p_{LC} , (d) the number of vertices s^3 .

Dataset		Odometry	Chordal	Spectral (Rotation Only)	Spectral	Global Opt.
Sphere	Iter	65	6	8	4	
	Cost	1.14×10^9	1971.17	5594.19	1742.75	1687
	Time (s)	-	0.707	0.602	0.779	
Torus	Iter	32	5	5	4	
	Cost	3.87×10^8	24669.2	25833.2	24272.7	24227
	Time (s)	-	1.316	1.501	1.199	
Grid	Iter	30	6	6	4	
	Cost	1.97×10^{10}	87252	86966.1	84486.4	84320
	Time (s)	-	8.747	18.806	0.25	
Garage	Iter	1028	3	4	4	
	Cost	2.31×10^9	1.42	3.215	2.7	1.26
	Time (s)	-	0.201	0.136	25.7	

Table 1: **Standard SLAM benchmarks** Objective value (cost) attained and computation time required for each initialization method on several SLAM benchmarks. We also report the number of iterations (Iter.) required for a Riemannian trust-region optimization method to converge to a critical point. Note that the reported computation time is only the time required to compute the initialization. Proposed approaches are **bold**.

(verifiably) globally optimal solutions; that is, these initialization methods coupled with standard *local* optimization techniques recovered globally optimal solutions *without* the need to explicitly solve a large-scale semidefinite program.

Both of the spectral methods (using the “full” pose-graph optimization data matrix \tilde{Q} and the “rotation only” version using only $L(\tilde{G}^p)$) provide estimates competitive with the state-of-the-art chordal initialization method, generally attaining near-optimal objective values.⁸ Interestingly, in their work, Moreira et al. [22] found that the rotation-only spectral estimator attains a higher cost on the Sphere dataset than alternative methods, as we do here; however, when we include the translation measurements, we find that this discrepancy disappears. Similarly, the chordal estimator also performs well on this dataset, despite the fact that, like the rotation-only spectral initialization, it does not make use of translational measurements.

7 Conclusion

In this work we presented the first initialization methods equipped with *explicit performance guarantees* adapted to the problems of pose-graph SLAM and rotation averaging. Our approach is based upon a simple *spectral relaxation* of the estimation problem, the form of which permits us to apply eigenvector perturbation bounds to control the distance from our initialization to *both* the (latent) ground-truth *and* the global minimizer of the estimation problem (the *maximum likelihood* estimate) as a function of the measurement noise. Consistent with recent complementary work on information-theoretic aspects [7, 12, 18] and global optimization methods [13, 14, 25] for SLAM and RA, our bounds highlight the central role that spectral properties of the measurement network⁹ play in controlling the accuracy of SLAM and RA solutions. Finally, we show experimentally that our spectral estimator is very effective in practice, producing initializations of

⁸Our current implementation is aimed at recovering high-precision eigenvector estimates, rather than expedient computation. Despite this, spectral initialization is often faster than the chordal approach, though occasionally this added precision leads to longer computation times than would be necessary to obtain a good estimate, e.g. on the Garage dataset.

⁹Specifically, the smallest nonzero eigenvalue $\lambda_{d+1}(Q)$, which can be thought of as a generalization of the algebraic connectivity of the classical graph Laplacian.

comparable or superior quality at lower computational cost compared to existing state-of-the-art techniques.

A Structure of the data matrices

In this appendix, we provide the definitions of the various matrices appearing in the parameterization of the rotation averaging and pose-graph SLAM problems. $L(W^\tau)$ and $L(W^\rho)$ denote the Laplacians of the translational weight graph $W^\tau \triangleq (\mathcal{V}, \mathcal{E}, \{\tau_{ij}\})$ and rotational weight graph $W^\rho \triangleq (\mathcal{V}, \mathcal{E}, \{\kappa_{ij}\})$, respectively, with *undirected edges* $\{i, j\} \in \mathcal{E}$. These are $n \times n$ matrices with i, j -entries:

$$L(W^\tau)_{ij} = \begin{cases} \sum_{e \in \delta(i)} \tau_e, & i = j, \\ -\tau_{ij}, & \{i, j\} \in \mathcal{E}, \\ 0, & \{i, j\} \notin \mathcal{E}, \end{cases} \quad (28a)$$

$$L(W^\rho)_{ij} = \begin{cases} \sum_{e \in \delta(i)} \kappa_e, & i = j, \\ -\kappa_{ij}, & \{i, j\} \in \mathcal{E}, \\ 0, & \{i, j\} \notin \mathcal{E}. \end{cases} \quad (28b)$$

$L(\tilde{G}^\rho)$ denotes the *connection Laplacian* for the rotational measurements, which is a $dn \times dn$ symmetric block-diagonal matrix with $d \times d$ blocks determined by:

$$L(\tilde{G}^\rho)_{ij} \triangleq \begin{cases} d_i^\rho I_d, & i = j, \\ -\kappa_{ij} \tilde{R}_{ij}, & \{i, j\} \in \mathcal{E}, \\ 0_{d \times d}, & \{i, j\} \notin \mathcal{E}, \end{cases} \quad (29a)$$

$$d_i^\rho \triangleq \sum_{e \in \delta(i)} \kappa_e, \quad (29b)$$

where $\delta(i)$ denotes the set of edges *incident to* node i . $\tilde{V} \in \mathbb{R}^{n \times dn}$ denotes the $(1 \times d)$ -block-structured matrix with (i, j) block given by:

$$\tilde{V}_{ij} \triangleq \begin{cases} \sum_{e \in \delta^-(j)} \tau_e \tilde{t}_e^\top, & i = j, \\ -\tau_{ji} \tilde{t}_{ji}^\top, & (j, i) \in \mathcal{E}, \\ 0_{1 \times d}, & \text{otherwise.} \end{cases} \quad (30)$$

Finally, $\tilde{\Sigma} \in \text{SBD}(d, n)$ denotes the symmetric block-structured diagonal matrix given by:

$$\begin{aligned} \tilde{\Sigma} &\triangleq \text{Diag}(\tilde{\Sigma}_1, \dots, \tilde{\Sigma}_n) \in \text{SBD}(d, n) \\ \tilde{\Sigma}_i &\triangleq \sum_{e \in \delta^-(i)} \tau_e \tilde{t}_e \tilde{t}_e^\top, \end{aligned} \quad (31)$$

where $\delta^-(i)$ denotes the set of edges *leaving* node i . With these definitions in hand, the translational data matrix \tilde{Q}^τ can be defined as:

$$\tilde{Q}^\tau = \tilde{\Sigma} - \tilde{V}^\top L(W^\tau) \tilde{V}. \quad (32)$$

B Analysis of the spectral relaxation

B.1 Recovering minimizers of Problem 4 as eigenvectors

In this section we derive a closed-form description of the *global* minimizers Y^* of the spectral relaxation Problem 4. Specifically, we prove the following theorem:

Theorem 7 (Global minimizers of the spectral relaxation). *Let $\lambda_1(\tilde{Q}) \leq \dots \leq \lambda_d(\tilde{Q})$ be the d smallest eigenvalues of \tilde{Q} . Then $Y^* \in \mathbb{R}^{d \times dn}$ is a global minimizer of the spectral relaxation Problem 4 if and only if*

$$Y^* = \sqrt{n} \begin{pmatrix} v_{\sigma(1)} \\ \vdots \\ v_{\sigma(d)} \end{pmatrix} \in \mathbb{R}^{d \times dn} \quad (33)$$

where $v_1, \dots, v_d \in \mathbb{R}^{dn}$ are a set of orthonormal eigenvectors corresponding to the d smallest eigenvalues, and σ is a permutation. The corresponding optimal value of Problem 4 is:

$$p_S^* = n \sum_{i=1}^d \lambda_i(\tilde{Q}). \quad (34)$$

Proof. Our approach will be to reduce Problem 4 to an equivalent problem whose critical points are already well-understood. To that end, let $Z \triangleq n^{-1/2} Y^\top \in \mathbb{R}^{dn \times d}$, so that $Y = \sqrt{n} Z^\top$. Substitution into Problem 4 then gives:

$$\begin{aligned} p_S^* &= \min_{Z \in \mathbb{R}^{dn \times d}} \operatorname{tr} \left(n \tilde{Q} Z Z^\top \right) \\ &\text{s.t. } Z^\top Z = I_d. \end{aligned} \quad (35)$$

Observe that $Z^\top Z = I_d$ if and only if $Z \in \operatorname{St}(d, dn)$; therefore, we may in turn rewrite (35) as the following *unconstrained* minimization over the Stiefel manifold:

$$p_S^* = \min_{Z \in \operatorname{St}(d, dn)} \operatorname{tr} \left(n \tilde{Q} Z Z^\top \right). \quad (36)$$

Note that we may now recognize (36) as the minimization of a generalized Rayleigh quotient over a Stiefel manifold. This problem has been extensively studied; in particular, Absil et al. [1, Section 4.8.2] provides an elementary proof that

$$Z = (z_1, \dots, z_d) \in \mathbb{R}^{dn \times d} \quad (37)$$

is a critical point of (36) *if and only if* its columns $\{z_i\}_{i=1}^d \subset \mathbb{R}^{dn}$ are an orthonormal set of eigenvectors for $n\tilde{Q}$. Moreover, substituting (37) into the objective in (35) and exploiting the fact that $\{z_i\}_{i=1}^d \subset \mathbb{R}^{dn}$ are pairwise mutually-orthogonal eigenvectors, we find that the corresponding objective value is:

$$\operatorname{tr} \left(n \tilde{Q} Z Z^\top \right) = n \sum_{i=1}^d \mu_i, \quad (38)$$

where μ_i is the eigenvalue corresponding to z_i . Since every critical point of (36) is of the form (37)–(38), it follows that the *global minimizers* Z^* are precisely those critical points whose columns are composed of the eigenvectors $v_1, \dots, v_d \in \mathbb{R}^{dn}$ corresponding to the d *smallest* eigenvalues of \tilde{Q} . Recovering the corresponding optimal Y^* from Z^* then gives (33) and (34). \square

B.2 Symmetric perturbations of symmetric matrices

Recall that \underline{R} and Y^* are solutions of the noiseless and noisy versions of the spectral relaxation in Problem 4. In Appendix B.1 we showed how these can be directly obtained from the Stiefel manifold elements giving the d minimum eigenvectors for their corresponding data matrices. The Davis-Kahan Theorem is a classical result in linear algebra that measures the perturbation of a matrix's eigenvectors under a symmetric perturbation of that matrix [28]. Therefore, we make use of this theorem to derive a bound on the estimation error of a spectral estimator as a function of the noise in the data matrix. In particular, the proof of Lemma 2 (and consequently Theorem 4) relies on a particular variant of the Davis-Kahan $\sin \theta$ Theorem [31, Theorem 2]. Here, we briefly restate the main result of [31] and give a proof of Lemma 2.

Theorem 8 (Yu et al. [31], Theorem 2). *Let $\Sigma, \hat{\Sigma} \in \mathbb{R}^{p \times p}$ be symmetric, with eigenvalues $\lambda_1 \leq \dots \leq \lambda_p$ and $\hat{\lambda}_1 \leq \dots \leq \hat{\lambda}_p$ respectively. Fix $1 \leq r \leq s \leq p$ and assume that $\min(\lambda_r - \lambda_{r-1}, \lambda_{s+1} - \lambda_s) > 0$, where $\lambda_0 \triangleq -\infty$ and $\lambda_{p+1} \triangleq \infty$. Let $d \triangleq s - r + 1$, and let $V = (v_r, v_{r+1}, \dots, v_s) \in \mathbb{R}^{p \times d}$ and $\hat{V} = (\hat{v}_r, \hat{v}_{r+1}, \dots, \hat{v}_s) \in \mathbb{R}^{p \times d}$ have orthonormal columns satisfying $\Sigma v_j = \lambda_j v_j$ and $\hat{\Sigma} \hat{v}_j = \hat{\lambda}_j \hat{v}_j$ for $j = r, r+1, \dots, s$. Then there exists an orthogonal matrix $G \in O(d)$ such that*

$$\|\hat{V}G - V\|_F \leq \frac{2^{3/2} \min(d^{1/2} \|\hat{\Sigma} - \Sigma\|_{op}, \|\hat{\Sigma} - \Sigma\|_F)}{\min(\lambda_r - \lambda_{r-1}, \lambda_{s+1} - \lambda_s)}. \quad (39)$$

With this result in hand, we are ready to prove Lemma 2.

Proof of Lemma 2. The data matrices \tilde{Q} and Q are symmetric $dn \times dn$ matrices with eigenvalues $\lambda_1 \leq \dots \leq \lambda_{dn}$ and $\tilde{\lambda}_1 \leq \dots \leq \tilde{\lambda}_{dn}$, respectively. From Theorem 7 we have that the d normalized eigenvectors corresponding to $\lambda_1, \dots, \lambda_d$ of Q and $\tilde{\lambda}_1, \dots, \tilde{\lambda}_d$ are exactly $n^{-1/2} \underline{R}^\top$ and $n^{-1/2} Y^{*\top}$, respectively. Then, letting $r = 1$ and $s = d$ and applying Theorem 8, there exists an orthogonal matrix $G \in O(d)$ such that:

$$\frac{1}{\sqrt{n}} \|Y^{*\top} G - \underline{R}^\top\|_F \leq \frac{2\sqrt{2d} \|\tilde{Q} - Q\|_2}{\lambda_{d+1}(Q) - \lambda_d(Q)}. \quad (40)$$

Multiplying both sides of this expression by \sqrt{n} , we have:

$$\|Y^{*\top} G - \underline{R}^\top\|_F \leq \frac{2\sqrt{2dn} \|\tilde{Q} - Q\|_2}{\lambda_{d+1}(Q) - \lambda_d(Q)}. \quad (41)$$

Now, by definition $\Delta Q = \tilde{Q} - Q$. If we assume \mathcal{G} is connected,¹⁰ from [25, Lemma 8] we have that $\lambda_{d+1}(Q) > 0$. Since $\underline{R} \in \ker(Q)$, we know that $\lambda_d(Q) = 0$ and the above expression simplifies to:

$$\|Y^{*\top} G - \underline{R}^\top\|_F \leq \frac{2\sqrt{2dn} \|\Delta Q\|_2}{\lambda_{d+1}(Q)}. \quad (42)$$

Taking the transpose of the terms inside the norm gives the desired result. \square

C Proof of the main results

In this appendix, we prove the main results, i.e. Theorem 4, Theorem 5, and Corollary 6.

¹⁰It is not particularly restrictive to assume that \mathcal{G} is connected. In the case that \mathcal{G} is not connected, the estimation problem splits over the connected components of \mathcal{G} , and all of our results hold separately for each connected component.

C.1 An upper bound for the estimation error in Problem 4

Proof of Theorem 4. To simplify the subsequent derivation, we will assume without loss of generality that \underline{R} and Y^* are the representatives of their orbits satisfying $d_{\mathcal{O}}(\underline{R}, Y^*) = \|\underline{R} - Y^*\|_F$. Recall from the definition of $d_{\mathcal{S}}(\underline{R}, R^{(0)})$ that:

$$d_{\mathcal{S}}(\underline{R}, R^{(0)}) = \min_{G \in \text{SO}(d)} \|\underline{R} - GR^{(0)}\|_F. \quad (43)$$

Therefore, we have:

$$\begin{aligned} d_{\mathcal{S}}(\underline{R}, R^{(0)})^2 &= \min_{G \in \text{SO}(d)} \|\underline{R} - GR^{(0)}\|_F^2 \\ &\leq \|\underline{R} - R^{(0)}\|_F^2, \\ &= \sum_{i=1}^n \|R_i - \Pi_{\mathcal{S}}(Y_i^*)\|_F^2, \end{aligned} \quad (44)$$

where in the last line we have used the fact that $R^{(0)}$ consists of the projections of individual $(d \times d)$ blocks of Y^* onto $\text{SO}(d)$. From Lemma 3, we have that each of the n summands above satisfies:

$$\|R_i - \Pi_{\mathcal{S}}(Y_i^*)\|_F^2 \leq 4\|R_i - Y_i^*\|_F^2. \quad (45)$$

This, in turn, gives a corresponding bound on the summation:

$$\begin{aligned} \sum_{i=1}^n \|R_i - \Pi_{\mathcal{S}}(Y_i^*)\|_F^2 &\leq 4 \sum_{i=1}^n \|R_i - Y_i^*\|_F^2 \\ &= 4\|\underline{R} - Y^*\|_F^2. \end{aligned} \quad (46)$$

Since, by hypothesis, Y^* and \underline{R} are representatives of their orbits satisfying $d_{\mathcal{O}}(\underline{R}, Y^*) = \|\underline{R} - Y^*\|_F$, we have:

$$4\|\underline{R} - Y^*\|_F^2 = 4d_{\mathcal{O}}(\underline{R}, Y^*)^2. \quad (47)$$

Applying Lemma 2, we directly obtain:

$$4d_{\mathcal{O}}(\underline{R}, Y^*)^2 \leq 4(2\sqrt{2dn})^2 \frac{\|\Delta Q\|_2^2}{\lambda_{d+1}(Q)^2}. \quad (48)$$

In summary, we have:

$$d_{\mathcal{S}}(\underline{R}, R^{(0)})^2 \leq 4(2\sqrt{2dn})^2 \frac{\|\Delta Q\|_2^2}{\lambda_{d+1}(Q)^2}. \quad (49)$$

Taking the square root of both sides of the inequality in the last line gives:

$$d_{\mathcal{S}}(\underline{R}, R^{(0)}) \leq \frac{4\sqrt{2dn}\|\Delta Q\|_2}{\lambda_{d+1}(Q)}, \quad (50)$$

which concludes the proof. \square

C.2 An upper bound for the estimation error in Problem 3

We begin following the arguments of Preskitt [23, Appendix D.4]. From the optimality of R^* we have:

$$\begin{aligned} \text{tr}(\tilde{Q}\underline{R}^\top \underline{R}) &= \text{tr}(\underline{Q}\underline{R}^\top \underline{R}) + \text{tr}(\Delta Q \underline{R}^\top \underline{R}) \\ &\geq \text{tr}(\underline{Q}R^{*\top} R^*) + \text{tr}(\Delta Q R^{*\top} R^*) = \text{tr}(\tilde{Q}R^{*\top} R^*). \end{aligned} \quad (51)$$

Since $\text{tr}(\underline{Q}\underline{R}^\top \underline{R}) = 0$, we can rearrange the above expression to obtain:

$$\text{tr}(\underline{Q}R^{*\top} R^*) \leq \text{tr}(\Delta Q \underline{R}^\top \underline{R}) - \text{tr}(\Delta Q R^{*\top} R^*). \quad (52)$$

Using the fact that $\text{tr}(\Delta Q \underline{R}^\top \underline{R}) = \text{vec}(\underline{R})^\top (\Delta Q \otimes I_n) \text{vec}(\underline{R})$ (and likewise for $\text{tr}(\Delta Q R^{*\top} R^*)$), we have:

$$\begin{aligned} \text{tr}(\underline{Q}R^{*\top} R^*) &\leq \text{vec}(\underline{R} - R^*)^\top (\Delta Q \otimes I_n) \text{vec}(\underline{R} + R^*) \\ &\leq \|\text{vec}(\underline{R} - R^*)\|_2 \|\Delta Q \otimes I_n\|_2 \|\text{vec}(\underline{R} + R^*)\|_2 \\ &= \|\underline{R} - R^*\|_F \|\Delta Q\|_2 \|\underline{R} + R^*\|_F \\ &\leq 2\sqrt{dn} \|\underline{R} - R^*\|_F \|\Delta Q\|_2. \end{aligned} \quad (53)$$

In order to lower-bound the right-hand side of (53) in terms of the estimation error $d_S(\underline{R}, R^*)$, we will make use of the following technical lemma of Rosen et al. [25]:

Lemma 9 (Lemma 11 of Rosen et al. [25]). *Let $R \in O(d)^n \subset \mathbb{R}^{d \times dn}$ and furthermore let $M = \{WR \mid W \in \mathbb{R}^{d \times d}\} \subset \mathbb{R}^{d \times dn}$ be the subspace of matrices with rows contained in $\text{image}(R^\top)$. Then*

$$\begin{aligned} \text{Proj}_V : \mathbb{R}^{dn} &\rightarrow \text{image}(R^\top) \\ \text{Proj}_V(x) &= \frac{1}{n} R^\top R x \end{aligned} \quad (54)$$

is the orthogonal projection onto $\text{image}(R^\top)$ with respect to the ℓ_2 inner product, and the map

$$\begin{aligned} \text{Proj}_M : \mathbb{R}^{d \times dn} &\rightarrow M \\ \text{Proj}_M(X) &= \frac{1}{n} X R^\top R \end{aligned} \quad (55)$$

which applies Proj_V to the rows of X is the orthogonal projection onto M with respect to the Frobenius inner product.

Since $\ker(Q) = \text{image}(\underline{R}^\top)$ and $\dim(\text{image}(\underline{R}^\top)) = d$, from Lemma 9, we have:

$$\text{tr}(\underline{Q}R^{*\top} R^*) \geq \lambda_{d+1}(\underline{Q}) \|P\|_F^2, \quad (56)$$

where

$$\begin{aligned} R^* &= K + P \\ K &= \text{Proj}_M(R^*) = \frac{1}{n} R^* \underline{R}^\top \underline{R} \\ P &= R^* - \text{Proj}_M(R^*) = R^* - \frac{1}{n} R^* \underline{R}^\top \underline{R} \end{aligned} \quad (57)$$

is an orthogonal decomposition of R^* and the rows of P are contained in the orthogonal complement of $\text{image}(\underline{R}^\top)$

The following lemma provides a bound on $d_S(\underline{R}, R^*)^2$ in terms of $\|P\|_F^2$.

Lemma 10. *Let R^* and \underline{R} be representatives of their orbits such that $d_{\mathcal{S}}(\underline{R}, R^*) = \|\underline{R} - R^*\|_F$, and $P = R^* - \text{Proj}_M(R^*)$ as defined in (57). Then:*

$$\frac{1}{4}d_{\mathcal{S}}(\underline{R}, R^*)^2 \leq \|P\|_F^2. \quad (58)$$

Proof. Let $X = \frac{1}{n}\underline{R}R^{*\top}$, so that $K = X^{\top}\underline{R}$. Expanding the left hand side, we have:

$$\begin{aligned} d_{\mathcal{S}}(\underline{R}, R^*)^2 &= \|R^* - \underline{R}\|_F^2 \\ &\leq \|R^* - \Pi_{\mathcal{S}}(X^{\top})\underline{R}\|_F^2, \end{aligned} \quad (59)$$

from the fact that the orbit distance is obtained as the minimum over $G \in \text{SO}(d)$ of the quantity $\|R^* - G\underline{R}\|_F$, and that by hypothesis this minimum is obtained as $\|R^* - \underline{R}\|_F$. Breaking up the norm into its blockwise summands, and from the orthogonal invariance of the Frobenius norm, we can rearrange this expression as follows:

$$\begin{aligned} \|R^* - \Pi_{\mathcal{S}}(X^{\top})\underline{R}\|_F^2 &= \sum_{i=1}^n \|R_i^* - \Pi_{\mathcal{S}}(X^{\top})R_i\|_F^2 \\ &= \sum_{i=1}^n \|R_i^*R_i^{\top} - \Pi_{\mathcal{S}}(X^{\top})\|_F^2. \end{aligned} \quad (60)$$

From Lemma 3, we know that each summand in the above expression satisfies

$$\|R_i^*R_i^{\top} - \Pi_{\mathcal{S}}(X^{\top})\|_F^2 \leq 4\|R_i^*R_i^{\top} - X^{\top}\|_F^2. \quad (61)$$

Since this bound is satisfied for each summand, the total summation satisfies

$$\begin{aligned} \sum_{i=1}^n \|R_i^*R_i^{\top} - \Pi_{\mathcal{S}}(X^{\top})\|_F^2 &\leq 4\sum_{i=1}^n \|R_i^*R_i^{\top} - X^{\top}\|_F^2 \\ &= 4\sum_{i=1}^n \|R_i^* - X^{\top}R_i\|_F^2 \\ &= 4\|R^* - X^{\top}\underline{R}\|_F^2. \end{aligned} \quad (62)$$

Since $K = X^{\top}\underline{R}$, we have:

$$\begin{aligned} 4\|R^* - X^{\top}\underline{R}\|_F^2 &= 4\|R^* - K\|_F^2 \\ &= 4\|P\|_F^2, \end{aligned} \quad (63)$$

which gives the desired bound. \square

With this result, we are ready to prove Theorem 5.

Proof. From (56) and (53), we have:

$$\lambda_{d+1}(Q)\|P\|_F^2 \leq 2\sqrt{dn}\|\underline{R} - R^*\|_F\|\Delta Q\|_2. \quad (64)$$

Since, by hypothesis, R^* and \underline{R} are the representatives of their orbits satisfying $d_{\mathcal{S}}(\underline{R}, R^*) = \|\underline{R} - R^*\|_F$, from Lemma 10 we have

$$d_{\mathcal{S}}(\underline{R}, R^*)^2 \leq 4\|P\|_F^2. \quad (65)$$

Combining (65) with (64), we obtain:

$$d_{\mathcal{S}}(\underline{R}, R^*) \leq \frac{8\sqrt{dn}\|\Delta Q\|_2}{\lambda_{d+1}(Q)}, \quad (66)$$

which is what we intended to show. \square

C.3 An upper bound on $d_{\mathcal{S}}(R^{(0)}, R^*)$

In this section, we give a proof of Corollary 6, bounding the $\text{SO}(d)^n$ orbit distance between the spectral initialization $R^{(0)}$ and the maximum likelihood estimate R^* . First, we establish as the main technical lemma a result that the orbit distances $d_{\mathcal{S}}$ and $d_{\mathcal{O}}$ on $\text{SO}(d)^n$ and $\text{O}(d)^n$ are *pseudometrics*:

Lemma 11 (Orbit distances are pseudometrics). *The orbit distances $d_{\mathcal{S}}$ and $d_{\mathcal{O}}$ are pseudometrics on $\text{SO}(d)^n$ and $\text{O}(d)^n$, respectively. In particular, for all $X, Y, Z \in \text{SO}(d)^n$, we have:*

1. $d_{\mathcal{S}}(X, X) = 0$
2. $d_{\mathcal{S}}(X, Y) = d_{\mathcal{S}}(Y, X)$
3. $d_{\mathcal{S}}(X, Z) \leq d_{\mathcal{S}}(X, Y) + d_{\mathcal{S}}(Y, Z)$,

and likewise for $d_{\mathcal{O}}$ on $\text{O}(d)^n$.

Proof. To simplify the subsequent derivation, we prove the result for the orbit distance $d_{\mathcal{S}}$ on $\text{SO}(d)^n$; the same argument applies *mutatis mutandis* to $d_{\mathcal{O}}$ on $\text{O}(d)^n$. A *pseudometric* on $\text{SO}(d)^n$ (resp. $\text{O}(d)^n$) is any nonnegative function $\text{SO}(d)^n \times \text{SO}(d)^n \rightarrow \mathbb{R}_{\geq 0}$ satisfying the properties 1–3 [17]. To establish 1, we have:

$$d_{\mathcal{S}}(X, X) = \min_{G \in \text{SO}(d)} \|X - GX\|_F = 0, \quad (67)$$

since $\|A\|_F \geq 0$ for all A and taking $G = I$ realizes this minimum value.

For 2, we have:

$$\begin{aligned} d_{\mathcal{S}}(X, Y) &= \min_{G \in \text{SO}(d)} \|X - GY\|_F \\ &= \min_{G \in \text{SO}(d)} \|Y - G^T X\|_F = d_{\mathcal{S}}(Y, X), \end{aligned} \quad (68)$$

where the second line follows from the orthogonal invariance of the Frobenius norm, and the last line follows from the fact that since $G^T = G^{-1} \in \text{SO}(d)$, then G^T ranges over all of $\text{SO}(d)$ as G does.

Finally, to establish 3, we aim to prove that for any $X, Y, Z \in \text{SO}(d)^n$:

$$d_{\mathcal{S}}(X, Z) \leq d_{\mathcal{S}}(X, Y) + d_{\mathcal{S}}(Y, Z). \quad (69)$$

Suppose the orbit distance $d_{\mathcal{S}}(X, Y)$ is attained with minimizer $G_{XY}^* \in \text{SO}(d)$ and likewise the distance $d_{\mathcal{S}}(Y, Z)$ is attained with minimizer $G_{YZ}^* \in \text{SO}(d)$. Define:

$$G' \triangleq G_{XY}^* G_{YZ}^*. \quad (70)$$

Now, since G' is itself the product of two elements of $\text{SO}(d)$, we know $G' \in \text{SO}(d)$, and therefore:

$$d_{\mathcal{S}}(X, Z) = \min_{G \in \text{SO}(d)} \|X - GZ\|_F \leq \|X - G'Z\|_F. \quad (71)$$

Examining the right-hand side of this expression, we have:

$$\begin{aligned} \|X - G'Z\|_F &= \|X - G_{XY}^* Y + G_{XY}^* Y - G'Z\|_F \\ &\leq \underbrace{\|X - G_{XY}^* Y\|_F}_{d_{\mathcal{S}}(X, Y)} + \|G_{XY}^* Y - G'Z\|_F, \end{aligned} \quad (72)$$

where the last line follows from the triangle inequality for the Frobenius norm. Now, substitution of the definition (70) into the second term of (72) reveals:

$$\begin{aligned} \|G_{XY}^* Y - G' Z\|_F &= \|G_{XY}^* Y - G_{XY}^* G_{YZ}^* Z\|_F \\ &= \|Y - G_{YZ}^* Z\|_F \\ &= d_S(Y, Z), \end{aligned} \tag{73}$$

where the second line follows from the orthogonal invariance of the Frobenius norm. Taken together, these results give:

$$d_S(X, Z) \leq \|X - G' Z\|_F \leq d_S(X, Y) + d_S(Y, Z), \tag{74}$$

which is what we intended to show. \square

Lemma 11 suggests a straightforward proof of Corollary 6.

Proof. From the triangle inequality for d_S , we have:

$$d_S(R^{(0)}, R^*) \leq d_S(R, R^{(0)}) + d_S(R, R^*). \tag{75}$$

Substitution of (23) and (24) into (75) gives the desired result. \square

D Relationship to the method of Moreira et al. [22]

In their recent work, Moreira et al. [22] also propose an estimator for pose-graph SLAM problems based on eigenvector computations. In this section, we show that their approach is formally equivalent to the *rotation-only* variant of the spectral initialization we discuss in Section 5 and therefore has estimation error satisfying the bound (27). Moreira et al. [22] specifically consider *unweighted* rotation measurements, which (from an estimation standpoint) is equivalent to considering the generative model (7) with *identical* precisions (say $\kappa_{ij} = 1$) for all edges $(i, j) \in \mathcal{E}$.

Their construction begins by considering the matrix $\tilde{M} \in \mathbb{R}^{dn \times dn}$ with $d \times d$ block i, j given by:

$$\tilde{M}_{ij} = \begin{cases} I_d & \text{if } i = j \\ \tilde{R}_{ij}, & \{i, j\} \in \mathcal{E} \\ 0_{d \times d} & \{i, j\} \notin \mathcal{E}. \end{cases} \tag{76}$$

They observe that for all stationary points $\hat{R} \in \text{SO}(d)^n \subset \mathbb{R}^{d \times dn}$, there is a corresponding matrix $\Lambda \in \mathbb{R}^{dn \times dn}$ such that:

$$\underbrace{(\Lambda - \tilde{M})}_{\tilde{S}} \hat{R}^\top = 0, \tag{77}$$

where Λ has the symmetric $d \times d$ block diagonal structure:

$$\Lambda = \begin{bmatrix} \Lambda_1 & \cdots & 0 \\ \vdots & \ddots & \vdots \\ 0 & \cdots & \Lambda_n \end{bmatrix}. \tag{78}$$

In the *noiseless* case where $\tilde{M} = \underline{M}$,¹¹ the matrix $\underline{S} = \Lambda - \underline{M}$ is given by [22, Equation 14]:

$$\underline{S} = (\mathcal{L} \otimes J_d) \circ \underline{M}, \tag{79}$$

¹¹In keeping with the notation in the rest of this manuscript, we use the notation \underline{M} to denote the measurement matrix (76) constructed from the *ground-truth* relative rotations R_{ij} .

where \mathcal{L} is the scalar (unweighted) rotational graph Laplacian with i, j entry:

$$\mathcal{L}_{ij} = \begin{cases} \delta(i), & i = j, \\ -1, & \{i, j\} \in \mathcal{E}, \\ 0, & \{i, j\} \notin \mathcal{E}, \end{cases} \quad (80)$$

$J_d \in \mathbb{R}^{d \times d}$ is an all-ones matrix, and \circ denotes the Hadamard product. Direct comparison of (80) with (28b) reveals that \mathcal{L} is equivalent to $L(W^\rho)$ when $\kappa_{ij} = 1$ for all $\{i, j\} \in \mathcal{E}$. Expanding (79), we have:

$$S_{ij} = \begin{cases} \delta(i)I_d, & i = j, \\ -R_{ij}, & \{i, j\} \in \mathcal{E}, \\ 0_{d \times d}, & \{i, j\} \notin \mathcal{E} \end{cases} \quad (81)$$

Comparing the definition of $L(\tilde{G}^\rho)$ in (29a) and S in (81), it is straightforward to verify that $S = L(G^\rho)$ when $\kappa_{ij} = 1$. From the equivalence of S and $L(G^\rho)$, it follows that $S \succeq 0$ and $R^\top \in \ker(S)$, so the ground-truth rotations R can be recovered by computing the d eigenvectors of S corresponding to the smallest eigenvalues of S .¹²

In the case of noisy measurements, Moreira et al. [22] propose to compute, as an approximation, the eigenvectors of $\tilde{S} = (\mathcal{L} \otimes J_3) \circ \tilde{M}$, which has $d \times d$ blocks given by:

$$S_{ij} = \begin{cases} \delta(i)I_d, & i = j, \\ -\tilde{R}_{ij}, & \{i, j\} \in \mathcal{E}, \\ 0_{d \times d}, & \{i, j\} \notin \mathcal{E}. \end{cases} \quad (82)$$

The justification given for this approximation is that, in the high signal-to-noise ratio regime, there ought to exist $R \in \text{SO}(d)^n$ such that $\tilde{S}R \approx 0$. Once again, however, directly comparing definitions reveals that the quantity $(\mathcal{L} \otimes J_3) \circ \tilde{M}$ is identical to $L(\tilde{G}^\rho)$ with $\kappa_{ij} = 1$ (cf. equations (82) and (29a)). Consequently, Moreira et al. [22]’s method is actually a *particular instance* of the spectral estimator we propose in Section 4, corresponding to the special case in which all rotational measurements have *equal weights* and the translational measurements have been discarded (i.e. the rotation-only case discussed in Section 5). Moreover, viewing this approach through the lens of the spectral relaxation in Problem 4 provides formal justification for the method and allows us to derive the explicit performance guarantees given in this paper.

References

- [1] P-A Absil, Robert Mahony, and Rodolphe Sepulchre. *Optimization Algorithms on Matrix Manifolds*. Princeton University Press, 2009.
- [2] Federica Arrigoni, Beatrice Rossi, and Andrea Fusiello. Spectral synchronization of multiple views in SE(3). *SIAM Journal on Imaging Sciences*, 9(4):1963–1990, 2016.
- [3] Afonso S Bandeira, Nicolas Boumal, and Amit Singer. Tightness of the maximum likelihood semidefinite relaxation for angular synchronization. *Mathematical Programming*, 163(1-2): 145–167, 2017.
- [4] Byron Boots and Geoff Gordon. A spectral learning approach to range-only SLAM. In *International Conference on Machine Learning*, pages 19–26. PMLR, 2013.

¹²Recall from Section 4 that R lie in $\ker(L(G^\rho))$ and from Section 3 that $L(G^\rho) \succeq 0$. The claim then follows from the equivalence of S and $L(G^\rho)$.

- [5] Nicolas Boumal. Nonconvex phase synchronization. *SIAM Journal on Optimization*, 26(4):2355–2377, 2016.
- [6] Nicolas Boumal, Amit Singer, and P-A Absil. Robust estimation of rotations from relative measurements by maximum likelihood. In *52nd IEEE Conference on Decision and Control*, pages 1156–1161. IEEE, 2013.
- [7] Nicolas Boumal, Amit Singer, P-A Absil, and Vincent D Blondel. Cramér–Rao bounds for synchronization of rotations. *Information and Inference: A Journal of the IMA*, 3(1):1–39, 2014.
- [8] Jesus Briales and Javier Gonzalez-Jimenez. Cartan-Sync: Fast and global SE(d)-synchronization. *IEEE Robotics and Automation Letters*, 2(4):2127–2134, 2017.
- [9] Luca Carlone, David M Rosen, Giuseppe Calafiore, John J Leonard, and Frank Dellaert. Lagrangian duality in 3D SLAM: Verification techniques and optimal solutions. In *2015 IEEE/RSJ International Conference on Intelligent Robots and Systems (IROS)*, pages 125–132. IEEE, 2015.
- [10] Luca Carlone, Roberto Tron, Kostas Daniilidis, and Frank Dellaert. Initialization techniques for 3D SLAM: a survey on rotation estimation and its use in pose graph optimization. In *2015 IEEE International Conference on Robotics and Automation (ICRA)*, pages 4597–4604. IEEE, 2015.
- [11] Luca Carlone, Giuseppe C Calafiore, Carlo Tommolillo, and Frank Dellaert. Planar pose graph optimization: Duality, optimal solutions, and verification. *IEEE Transactions on Robotics*, 32(3):545–565, 2016.
- [12] Yongbo Chen, Shoudong Huang, Liang Zhao, and Gamini Dissanayake. Cramér–Rao bounds and optimal design metrics for pose-graph SLAM. *IEEE Transactions on Robotics*, 37(2):627–641, 2021.
- [13] Frank Dellaert, David M Rosen, Jing Wu, Robert Mahony, and Luca Carlone. Shonan rotation averaging: Global optimality by surfing $SO(p)^D$. In *European Conference on Computer Vision*, pages 292–308. Springer, 2020.
- [14] Taosha Fan, Hanlin Wang, Michael Rubenstein, and Todd Murphey. CPL-SLAM: Efficient and certifiably correct planar graph-based SLAM using the complex number representation. *IEEE Transactions on Robotics*, 36(6):1719–1737, 2020.
- [15] Giorgio Grisetti, Rainer Kummerle, Cyrill Stachniss, and Wolfram Burgard. A tutorial on graph-based SLAM. *IEEE Intelligent Transportation Systems Magazine*, 2(4):31–43, 2010.
- [16] Richard J Hanson and Michael J Norris. Analysis of measurements based on the singular value decomposition. *SIAM Journal on Scientific and Statistical Computing*, 2(3):363–373, 1981.
- [17] John L Kelley. *General Topology*. Van Nostrand, New York, 1955.
- [18] Kasra Khosoussi, Shoudong Huang, and Gamini Dissanayake. Novel insights into the impact of graph structure on SLAM. In *2014 IEEE/RSJ International Conference on Intelligent Robots and Systems*, pages 2707–2714. IEEE, 2014.
- [19] Shuyang Ling. Near-optimal performance bounds for orthogonal and permutation group synchronization via spectral methods. *arXiv preprint arXiv:2008.05341*, 2020.

- [20] Huikang Liu, Man-Chung Yue, and Anthony Man-Cho So. A unified approach to synchronization problems over subgroups of the orthogonal group. *arXiv preprint arXiv:2009.07514*, 2020.
- [21] Daniel Martinec and Tomas Pajdla. Robust rotation and translation estimation in multiview reconstruction. In *2007 IEEE Conference on Computer Vision and Pattern Recognition*, pages 1–8. IEEE, 2007.
- [22] Gabriel Moreira, Manuel Marques, and Joao Paulo Costeira. Fast Pose Graph Optimization via Krylov-Schur and Cholesky Factorization. In *Proceedings of the IEEE/CVF Winter Conference on Applications of Computer Vision*, pages 1898–1906, 2021.
- [23] Brian Patrick Preskitt. *Phase retrieval from locally supported measurements*. PhD thesis, UC San Diego, 2018.
- [24] Yixuan Qiu. Spectra: C++ library for large scale eigenvalue problems. <https://spectralib.org>, 2015.
- [25] David M Rosen, Luca Carlone, Afonso S Bandeira, and John J Leonard. SE-Sync: A certifiably correct algorithm for synchronization over the special Euclidean group. *The International Journal of Robotics Research*, 38(2-3):95–125, 2019.
- [26] David M Rosen, Kevin J Doherty, Antonio Terán Espinoza, and John J Leonard. Advances in Inference and Representation for Simultaneous Localization and Mapping. *Annual Review of Control, Robotics, and Autonomous Systems*, 4, 2021.
- [27] Amit Singer. Angular synchronization by eigenvectors and semidefinite programming. *Applied and computational harmonic analysis*, 30(1):20–36, 2011.
- [28] G.W. Stewart, J.W. Stewart, J. Sun, Academic Press (Londyn)., and Harcourt Brace Jovanovich. *Matrix Perturbation Theory*. Computer Science and Scientific Computing. Elsevier Science, 1990. ISBN 9780126702309.
- [29] Yulun Tian, Kasra Khosoussi, David M Rosen, and Jonathan P How. Distributed certifiably correct pose-graph optimization. *arXiv preprint arXiv:1911.03721*, 2019.
- [30] Shinji Umeyama. Least-squares estimation of transformation parameters between two point patterns. *IEEE Transactions on Pattern Analysis & Machine Intelligence*, 13(04):376–380, 1991.
- [31] Yi Yu, Tengyao Wang, and Richard J Samworth. A useful variant of the Davis–Kahan theorem for statisticians. *Biometrika*, 102(2):315–323, 2015.